CAMBRIDGE
UNIVERSITY PRESS

Article

Optimized chemical preconditioning of Philippine natural zeolites

Eleanor M. Olegario[1], Kathrina Lois M. Taaca[1]* (iD), John Christopher Lawrence Morillo[2] and Herman D. Mendoza[1]

[1]Department of Mining, Metallurgical, and Materials Engineering, College of Engineering, University of the Philippines Diliman, Quezon City, 1100 Philippines and [2]Environmental Monitoring Laboratory, National Institute of Geological Sciences, University of the Philippines Diliman, Quezon City, 1100 Philippines

Abstract

Natural zeolites in the Aksitero sedimentary formation of the western Luzon area of the Philippines were evaluated. The natural washed zeolite (NW-Z) was preconditioned with acid to purify it and increase its surface area. Acid treatment with 3 M HCl for 12 h yielded optimum acid treatment of the NW-Z, causing increases in the Si/Al ratio, the specific surface area by 32.5% and the porosity of the acid-treated zeolite (HC-Z). The HC-Z was washed with 4 M NaCl for 3, 6, 12, 18, 24, 48 and 72 h to improve its cation-exchange capacity for copper. The sodium-treated zeolite (Na-Z) was immersed in 100 ppm CuSO$_4$ solution to test the copper-uptake capacity. Pretreatment of HC-Z with 4 M NaCl for 24 h is optimal for sodium treatment of the preconditioned HC-Z. The preconditioning techniques did not significantly alter the structure and morphology of the zeolite samples. It is suggested that the preconditioned Philippine natural zeolite samples are readily available for further functionalization that will enhance their antibacterial, catalytic and adsorption properties, with various useful applications in the field of catalysis, biomedicine, environmental mitigation and wastewater treatment.

The Late Eocene to Early Oligocene age Aksitero formation is the oldest sedimentary formation in the West Central Luzon basin of the Philippines, which serves as the sedimentary capping to the Zambales ophiolite (Yumul & Dimalanta, 1997), a complete sequence of oceanic crust and upper-mantle rocks. It is situated close to Tarlac, Zambales and Pangasinan areas and has two recognizable members: the Bigbiga Limestone member and the Burgos member. The Bigbiga Limestone member is in the lower section of the Aksitero formation and consists of micritic limestones intercalated with tuffaceous turbidites. The Burgos member, on the other hand, occurs in the upper section of the Aksitero formation, consisting of interbedded limestone, calcareous–tuffaceous turbidity sandstones, siltstones and mudstones. Petrographic analyses of the limestones and turbidites in the Aksitero formation were conducted to determine the origin and diagenetic processes undergone by the sedimentary units. The hemipelagic limestones predominantly contain fragments of planktonic foraminifera and nanofossils, with evidence of replacements of the original micritic tests by cristobalite, zeolite (clinoptilolite and mordenite) and smectite, which suggest volcanic origins. The tuffaceous turbidites, on the other hand, have graded textures and beds showing complete Bouma sequences, and thus signify transport and re-deposition from turbidity currents (Garrison et al., 1979).

Exposed portions of the Burgos member of the Aksitero formation were also investigated in the SAILE mine located in Mangatarem, Pangasinan. SAILE Industries, Inc., is the only commercial producer of natural zeolite and bentonite mineral products in the Philippines with a Mineral Production Sharing Agreement issued by the Mines and Geosciences Bureau under the Department of Environment and Natural Resources in the Philippines. The samples collected from the mine site show beds of zeolite (clinoptilolite), bentonite and silica occurring in the turbiditic layers. Zeolitized layers, consisting particularly of clinoptilolite and mordenite, are common, occurring as cement or as secondary mineral precipitates in voids. Zeolitization was caused by burial diagenesis at depths of ∼3.5–4.0 km and geothermal gradients of 15–20°C km^{-1} (Garrison et al., 1979). The possible depositional settings included submarine eruption and gravity flows aided by turbidity currents that eventually transported sediments away from the vent towards a deeper basinal area, where calcareous hemipelagic ooze dominated (Garrison et al., 1979).

An alternative mechanism related the zeolite genesis in the Aksitero formation with the hyper-alkaline Manleluag hot springs (pH 10.0–11.5) in Mangatarem, Pangasinan (Vargas et al., 2009; Arcilla et al., 2011). The high pH of the hot spring is due to the hydrolysis of Mg-rich rocks (gabbros) and Fe hydrolysis and oxidation of the pyroxenes present in the Zambales ophiolite. The hyper-alkaline waters from this reaction may have dissolved silica, which re-precipitated at lower temperatures, leading to zeolite formation (Vargas et al., 2009; Arcilla et al., 2011).

The Philippine natural zeolites (PNZs), consisting primarily of clinoptilolite and mordenite, are currently mined and used in applications including heavy metal removal (Cagomoc & Vasquez Jr, 2016; Olegario-Sanchez & Pelicano, 2017), nanotechnology (Olegario et al., 2019a, 2019b), oil removal (Osonio & Olegario-Sanchez, 2017), wastewater treatment (Barola et al., 2019; Dignos et al., 2019) and, more recently, biomedical

applications (Olegario-Sanchez & Felizco, 2017; Olegario-Sanchez *et al.*, 2017; Osonio & Vasquez Jr, 2018; Taaca & Vasquez Jr, 2018). Locally sourced natural zeolites remain largely unexploited in such applications due to variation in the purity and composition of the various deposits. In addition, the availability and versatility of synthetic zeolites have inhibited the commercialization of natural zeolites. However, the PNZs have already been utilized as raw materials for animal feeds, agricultural stocks and other industrial applications in the local market. Recently, they have been used for inactivation of *Escherichia coli* (Olegario-Sanchez *et al.*, 2017) and as noble-metal catalytic converters (Guerrero *et al.*, 2019) after modification with Cu. Nevertheless, both synthetic and natural zeolites have attracted growing interest regarding their use in various applications that involve ion-exchange processes.

To maximize the ion-exchange capacity of PNZ samples, preconditioning treatments should be performed. Preconditioning of zeolites has been carried out in the past to enhance their ion-exchange capacity (Ndayambaje, 2011), although the methods applied may not be optimal for locally sourced zeolites. These modifications include acid treatment, de-alumination and de-cationization, ion exchange and thermal treatment. The processes remove cations from the zeolite structure and transform zeolites in a near-homoionic form with increased content of the target cation (Semmens *et al.*, 1988; Ndayambaje, 2011). Various conditioning techniques, however, may affect the ion-exchange behaviour of natural zeolites (Cerjan-Stefanović *et al.*, 1996). The effects of NaCl, KCl and HCl were studied to evaluate the Cu^{2+} and Co^{2+} removal efficiency of South African clinoptilolite samples in column experiments (Mamba *et al.*, 2010). The HCl-conditioned clinoptilolite was the most efficient in terms of metal removal (Mamba *et al.*, 2009). In a similar study, Na-treated zeolites displayed excellent selectivity for Zn^{2+} followed by Mn^{2+}, compared to unconditioned natural zeolites (Cerjan-Stefanović *et al.*, 1996).

Among the conditioning agents, HCl has been reported to be an effective agent for improving the ion-exchange capacity of natural zeolites. In addition, HCl leaches Al^{3+} out of the clinoptilolite structure (Mamba *et al.*, 2010). Moreover, Na treatment may replace certain cations on the zeolite framework, rendering it homoionic. The Na^+ ions are easily exchanged in the zeolite structure, which greatly affects the exchange properties of zeolite (Semmens *et al.*, 1988). Thus, the present work aims to observe the influence of a two-step preconditioning treatment of PNZ on the morphology, texture and structural properties of the PNZ samples. The PNZ samples were first acid conditioned using HCl, followed by Na^+ exchange. For each step, the best-conditioned samples were used. The cation-exchange capacity and selectivity of the PNZ samples were assessed by ion exchange of PNZ with Cu^{2+} ions.

Experimental

Sample preparation

A total of 200 g of PNZ tuffaceous rock samples was obtained from the SAILE Mine in Mangatarem, Pangasinan. The samples were crushed and sieved to particle sizes of 1 and 3 mm. Granules were washed four times with deionized (DI) water and sun dried for 48 h. Further drying was performed prior to acid treatment by oven drying of the natural washed zeolites (NW-Z) at 150°C for 6 h.

Table 1. Factors and levels for the 2^3 factorial experimental design.

Factors	Parameter coding	Low level	High level
HCl concentration (M)	A	1	3
Soaking time (h)	B	6	12
Particle size (mm)	C	1	3

Preconditioning of the PNZ samples

Acid pretreatment of the PNZ samples

HCl preconditioning treatment. The NW-Z samples were soaked in HCl solutions (20% w/v) (Sigma Aldrich). The NW-Z powders were soaked in 1 M and 3 M HCl concentrated solutions for 6 and 12 h. Acid-treated zeolite (HC-Z) samples were washed 12 times with DI water until the pH of the supernatant was 6–7. Chlorine strips were also used as indicators to ensure that the zeolites were Cl⁻ free.

Experimental design. The HC-Z samples were prepared by varying the preparation variables, namely HCl concentration, soaking time and particle size, represented as A, B and C, respectively, using a 2^3 factorial experimental design. The experimental levels and the range of the variables are listed in Table 1. The Si/Al ratio calculated from atomic absorption spectrometry (AAS) analyses was selected as the response variable. Each factor was examined at two levels: 1 M and 3 M for A, 6 and 12 h for B and 1 and 3 mm for C. The design of the study had eight different experimental conditions. Table 2 presents the series of trials of the 2^3 factorial design. A total of 16 runs were performed in this study, with each experimental condition conducted in duplicate. The results of the experiment were analysed with *MINITAB* software. The analysis of variance (ANOVA) results for this design are presented in Table 3.

Chemical conditioning of the acid-pretreated samples

Na^+ exchange. Two sets of optimization conditions were used for the Na^+ ion exchange of 10% w/v HC-Z samples. The first optimization condition is focused on determining the best NaCl (99% Salinas) concentration (1 M, 2 M and 4 M) for the preconditioning of HC-Z samples at room temperature for 24 h. The second optimization condition used the best constant NaCl concentration

Table 2. Trials of the 2^3 factorial experimental design with the Si/Al ratio as the response variable.

Trial	HCl concentration (A, M)	Soaking time (B, h)	Particle size (C, mm)	Si/Al ratio
1	1	12	3	6.52
2	3	6	1	8.29
3	1	12	1	7.11
4	3	6	3	6.78
5	3	6	3	7.17
6	1	6	3	5.90
7	3	6	1	7.30
8	1	12	1	6.72
9	3	12	3	7.39
10	3	12	1	8.40
11	3	12	3	7.90
12	1	6	1	6.98
13	1	12	3	6.82
14	1	6	1	6.60
15	3	12	1	7.77
16	1	6	3	6.57

Table 3. ANOVA results for the 2^3 factorial experimental design.

Source	Sum of squares	Degrees of freedom	Mean square	F-value	Prob > F (p-value)
Model	5.634675	7	0.804954	4.907131	0.019883
A	3.783025	1	3.783025	23.06195	0.001352
B	0.5776	1	0.5776	3.521146	0.097433
C	1.0609	1	1.0609	6.467424	0.034543
AB	0.04	1	0.04	0.243847	0.634712
AC	0.0529	1	0.0529	0.322487	0.585697
BC	0.119025	1	0.119025	0.725596	0.419082
ABC	0.001225	1	0.001225	0.007468	0.933259
Pure error	1.3123	8	0.164038		
Corrected total	6.946975	15			

to determine the best soaking time between 3, 6, 12, 18, 24, 48 and 72 h. The Na-Z samples were thoroughly washed with DI water until Cl^- free ($AgNO_3$ test). The filtered Na-Z samples were dried at 150°C for 6 h.

Characterization

Optimization was conducted to ensure utilization of the best pre-treated samples (HCl and NaCl conditioning steps) before the Cu^{2+} ion exchange. Thus, this study assessed the as-prepared sample (NW-Z), the optimized acid-pretreated sample (HC-Z) and the Na^+-exchanged zeolite sample (Na-Z). The Si/Al ratio for the optimization of HCl pretreatment as well as the saturation percentage of the Na^+ loading were determined via AAS (Shimadzu AA-7000) at the Institute of Chemistry of the University of the Philippines Diliman (UP Diliman). Calibration for the AAS analysis was performed using a suitable calibration curve. The porosity and specific surface area of the untreated PNZ and HC-Z samples were determined using the Brunauer–Emmett–Teller (BET) method using Micromeritics Tristar II Plus equipment. The equipment utilized CO_2 and N_2 isotherms to calculate the pore-size diameter of the materials. CO_2 was used for porosity measurement and N_2 was used for surface area determination at 273 and 77 K, respectively. The samples were degassed at 90°C and 350°C for 2 and 8 h, respectively, with a ramp rate of 10°C min^{-1}. Data analysis was performed using *MicroActive* version 2.02 software. The Cu^{2+} uptake of zeolite was determined using microwave plasma-atomic emission spectroscopy (Agilent 4200). The chemical functional groups were detected by Fourier-transform infrared (FTIR; Nicolet MAGNA-IR 560) spectroscopy with a diffuse reflectance spectroscopy accessory. The zeolite phases of the samples were identified by X-ray diffraction (XRD; Shimadzu XRD-7000) operated at 40 kV and 30 mA with Cu-$K\alpha$ radiation in the range 2–80°2θ at the National Institute of Geological Sciences, UP Diliman. The surface morphology of the samples was determined with scanning electron microscopy (SEM) using a Shimadzu SSX-550 SEM equipped with an energy-dispersive spectrometer (EDX; JEOL JSM 5300) at the Engineering Department of Hokkaido University (Japan). The composition of the samples was determined using the EDX.

Results and discussion

Preconditioning of PNZ

Acid conditioning of PNZ
Statistical analysis. The results of the statistical analysis are shown in Table 2. The Si/Al ratios of the synthesized HC-Z samples
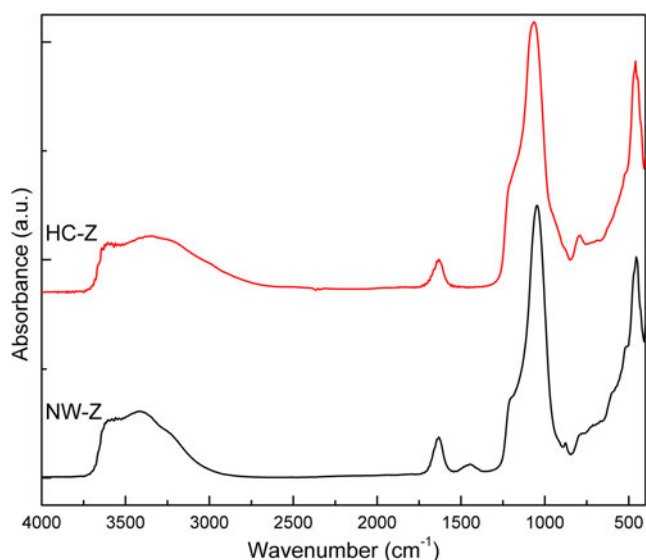
Fig. 1. FTIR spectra of the NW-Z and HC-Z samples.

ranged from 5.9 to 8.4. Table 3 summarizes the main results of the statistical analysis using ANOVA. The HCl concentration and particle size affect significantly the Si/Al ratio of the zeolite samples because they have p-values of <0.05. Moreover, these factors do not significantly influence each other, as evidenced by the high p-values (>0.1) for all interactions. In contrast, the soaking time (factor B) has a p-value of >0.05. Hence, the optimum acid pretreatment condition to be used in this study is to soak NW-Z samples with a particle size of 1 mm in a 3 M HCl solution for 12 h.

FTIR analysis of NW-Z and HC-Z samples. FTIR spectroscopy was employed to determine the functional groups present in the zeolite samples, as well as to ascertain that the Al–Si (both represented as T) cage of the samples remains intact after acid preconditioning. Characteristic zeolite bands were observed in the 400–1800 cm^{-1} range (Fig. 1) (Gligor *et al.*, 2010). The strong bands at 455 and 1042 cm^{-1} represent the O–T–O angular deformation and T–O asymmetric external stretching, respectively, of the NW-Z sample. Characteristic bands at 798, 1439 and 1620 cm^{-1} correspond to the T–O external symmetric stretching, T–O asymmetric internal stretching and H–O–H angular deformation of adsorbed water, respectively. The broad band at 3400 cm^{-1} is attributed to the O–H bond stretching of adsorbed water molecules in the NW-Z sample (Taaca & Vasquez Jr, 2017).

The bands at 400–1200 cm^{-1} were enlarged, and these are shown in Fig. 2. There are slight shifts in the characteristic bands of NW-Z after the acid preconditioning. The positions of the shifted bands are summarized in Table 4. This effect of the acid pretreatment may be an indication of degradation to the zeolite framework (Ndayambaje, 2011).

Chemical composition of the zeolite samples. Table 5 lists the chemical compositions of the NW-Z and HC-Z samples obtained by EDX analysis. During acid pretreatment, most cations were leached from the HC-Z. The Si/Al ratios are 4.90 for the NW-Z samples and 7.48 for the HC-Z samples. The change in the cation and Si/Al content of the PNZs is due to proton attack at the Al sites. Al–OH or cationic Al–OM bonds can be a result of proton attack
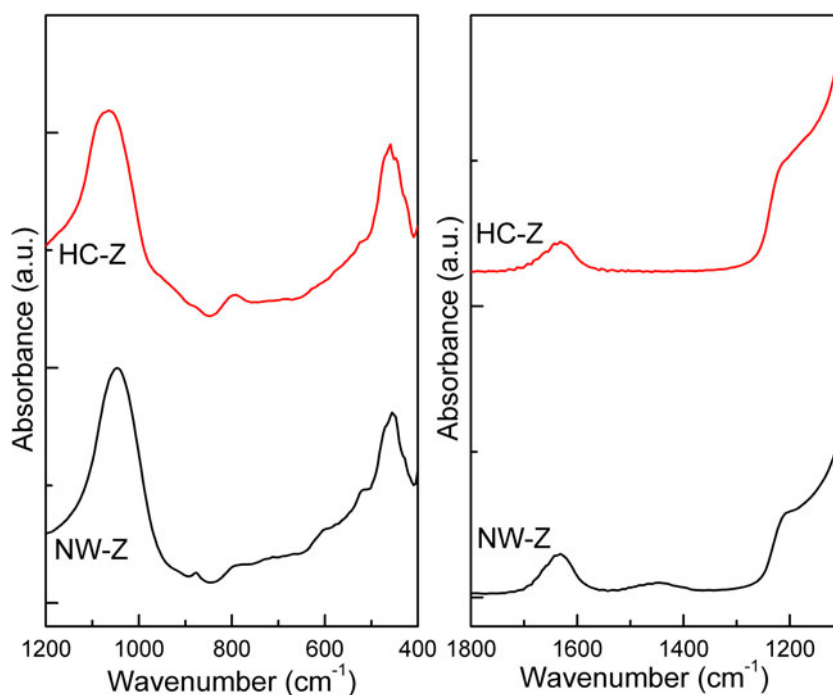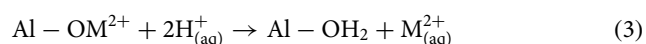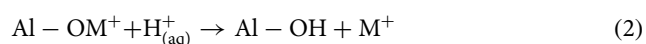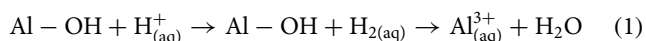
Fig. 2. FTIR spectra of the NW-Z and HC-Z samples in the 1200–400 and 2200–1200 cm^{-1} range.

at the Al sites (Cakicioglu-Ozkan, 2010). The possible reaction mechanisms that caused the de-alumination and affected the Si/Al ratio of the PNZs are described in equations 1–3. Aluminium dissolution in the PNZ samples occurred upon soaking in the HCl solution. This was associated with adsorption of protons at the cationic sites close to the Al sites and removal of any monovalent (M^+) or bivalent (M^{2+}) cations at the zeolite edges (Doula & Ionnou, 2003).

$$Al - OH + H^+_{(aq)} \rightarrow Al - OH + H_{2(aq)} \rightarrow Al^{3+}_{(aq)} + H_2O \quad (1)$$

$$Al - OM^+ + H^+_{(aq)} \rightarrow Al - OH + M^+ \quad (2)$$

$$Al - OM^{2+} + 2H^+_{(aq)} \rightarrow Al - OH_2 + M^{2+}_{(aq)} \quad (3)$$

Specific surface area and pore-size distribution. The specific surface area and pore-size distribution of the zeolite samples before and after acid pretreatment were determined by BET analysis. The N_2 adsorption isotherms of the HC-Z samples are of type 1 according to the International Union of Pure and Applied Chemistry (IUPAC) classification. Changes in the specific surface area and porosity (pore volume and pore size) of the PNZ

samples were detected using the adsorption isotherm data evaluated using the t-plot, Langmuir and Dubinin–Astakhov methods (Table 6). The specific surface area and pore volume of the HC-Z samples increased by 62% and 32%, respectively, relative to the PNZ samples. The increases in the micropore volume and specific surface area are attributed to the formation of secondary micropores that are larger than the main pore system (7–20 Å) due to the opening of pockets on the zeolite (Cakicioglu-Ozkan, 2010; Hernandez, 2014). The increased specific surface area and porosity of the HC-Z samples may be due to the increased open spaces in the zeolite framework. The SEM-EDX results show that most cations were removed or redistributed within the zeolite framework (Table 5).

The nature of the acid used affects the structure of zeolite because ligands (L) such as Cl^- ions form complexes on the zeolite surface. The Al or Si atoms (represented as T) on the zeolite surfaces are centres for the formation of outer-sphere complexes on the protonated zeolite surface ($T-OH^{2+}$) with the ligands (L^{n-}), as shown in equation 4. The use of HCl led to adsorption on the external surface to form outer-sphere complexes that follow the ion-exchange reactions shown in equations 4 and 5. Equation 5 shows the formation of inner-sphere complexes on

Table 4. Characteristic FTIR bands (cm^{-1}) of the NW-Z and HC-Z samples.

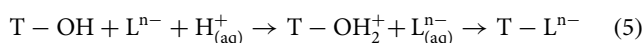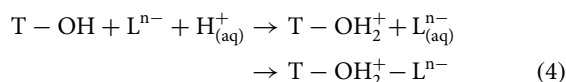| Vibration mode	NW-Z	HC-Z
O–T–O angular deformation	455	463
T–O external symmetric stretching	798	791
T–O asymmetric external stretching	1042	1065
T–O asymmetric internal stretching	1439	–
H–O–H angular deformation	1620	1636
O–H bond stretching	3410 and 3603	3364 and 3615

Table 5. SEM-EDX analyses of the composition (wt.%) of the NW-Z and HC-Z samples.

Analyte	NW-Z	HC-Z
SiO_2	67.21	77.69
Al_2O_3	13.61	10.53
FeO	9.63	6.59
CaO	2.51	1.20
K_2O	1.58	0.46
TiO_2	1.16	0.36
MgO	2.59	1.66
MnO	0.18	0.16
Na_2O	1.53	1.35

Table 6. Specific surface area and porosity of the NW-Z and HC-Z samples.

Parameter	NW-Z	HC-Z
Specific surface area (m^2 g^{-1})	116	189
Pore volume (cm^3 g^{-1})	0.041	0.050
Pore size (Å)	13	10

the protonated sites of zeolite (Doula & Ionnou, 2003).

$$T - OH + L^{n-} + H^+_{(aq)} \rightarrow T - OH_2^+ + L^{n-}_{(aq)}$$
$$\rightarrow T - OH_2^+ - L^{n-} \qquad (4)$$

$$T - OH + L^{n-} + H^+_{(aq)} \rightarrow T - OH_2^+ + L^{n-}_{(aq)} \rightarrow T - L^{n-} \qquad (5)$$

As a result, the use of HCl can improve the properties of the external surface and facilitate the extraction of Al atoms. It is also very effective at increasing the size of the micropores (pore volume) of the PNZs without destroying their crystal structure (Cakicioglu-Ozkan & Ulku, 2005). This, in turn, indicates that the use of HCl for preconditioning treatment is effective for producing more porous adsorbents.

Na$^+$ conditioning of the HC-Z samples

After acid pretreatment, Na$^+$ ions should be introduced to the zeolite that has had free pore spaces formed inside it and on its surface by the acid pretreatment. The cation-exchange capacity (CEC) of zeolite is improved by rendering the zeolite homoionic via Na$^+$ pretreatment (Ndayambaje, 2011). The HC-Z samples were soaked under various conditions to determine the best concentration to use, as well as the best soaking time. Then, the dried Na-Z samples were soaked with a Cu solution to exchange Na$^+$ ions with Cu^{2+} ions. The Cu^{2+} ion was chosen because further functionalization of the PNZs may include Cu modification for bacteria inactivation (Olegario-Sanchez et al., 2017). The amount of Cu^{2+} ions in the eluate was determined by AAS. A small Cu^{2+} content in the eluate would indicate that most of the Na$^+$ ions were displaced by the Cu^{2+} ions.

The results of the Cu^{2+} exchange are listed in Table 7. After 24 h, the eluates of the Na-Z samples treated with a 4 M NaCl concentration contained the smallest number of Cu^{2+} ions, corresponding to a Cu uptake of 99.88%. Although the Cu uptake values of the Na-Z samples do not differ greatly, increasing the Na$^+$ concentration may also increase the amount of Cu^{2+} ions adsorbed by the zeolite.

Figure 3 shows the optimized soaking time of Na-Z samples treated at a 4 M concentration, determined by the Cu^{2+} uptake (%) from aqueous solutions containing 100 ppm CuSO$_4$. The initial Cu^{2+} uptake observed on the Na-Z samples soaked for 3 h was 84.87%, which increased to 88.72% and 90.50% in the Na-Z

Table 7. Cu uptake (%) for the Na-Z samples modified with various concentrations of NaCl.

Zeolite modification	Cu uptake
Na-Z (1 M NaCl)	99.69
Na-Z (2 M NaCl)	99.81
Na-Z (4 M NaCl)	99.88
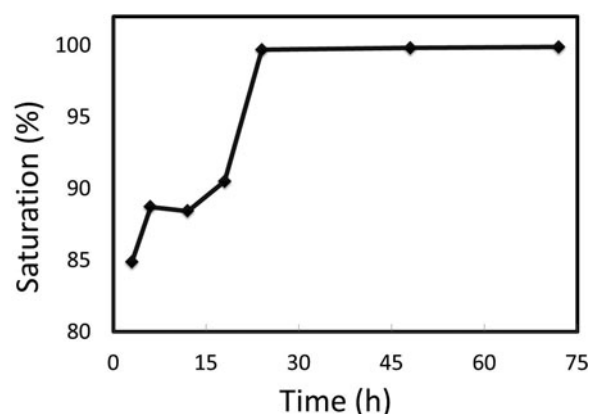
Fig. 3. Saturation *vs.* soaking time of Na-Z samples in 1 M CuSO$_4$ for 3, 6, 12, 18, 24, 48 and 72 h.

samples soaked for 6 and 18 h, respectively. After 24 h, the Na-Z samples had adsorbed 99.69% of the Cu^{2+} ions in the Cu solution, which remained constant even after soaking for 48 and 72 h. Hence, the Na-Z samples displayed maximal Na$^+$ adsorption after immersion in the NaCl solution for 24 h. Furthermore, PNZ samples have shown maximal Cu uptake at 24 h in previous studies (Olegario-Sanchez et al., 2017).

Cu^{2+} loading comparison between the NW-Z, HC-Z and Na-Z samples

Table 8 shows the Cu uptake percentages of the various PNZ samples in this work. The NW-Z samples displayed 99.40% Cu^{2+} uptake, indicating that Ca^{2+}, K$^+$, Na$^+$ and Mg$^+$ exchangeable cations detected by ED-XRF analysis (Table 5) are exchanged with Cu^{2+} ions. The HC-Z displayed a lower Cu uptake (96.62%), indicating a lower CEC for Cu^{2+} ions. Finally, the Na-Z samples yielded the greatest Cu^{2+} uptake (99.88%), which, although comparable to the Cu uptake of NW-Z, shows that the presence of exchangeable Na$^+$ ions enhances the Cu adsorption capacity of the zeolite, as ion exchange is the mechanism of adsorption. In addition, the Na-Z samples showed improved textural properties compared to the NW-Z samples due to the acid conditioning step. The NW-Z material still contains impurities, similar to the starting PNZ material.

Structural and morphological analyses of the zeolite samples

Phase structure identification of the zeolite samples. The XRD traces of the NW-Z, HC-Z, Na-Z and Cu-Z samples are shown in Fig. 4. The major phase of PNZs is clinoptilolite (C), with minor mordenite (M), quartz (Q) and feldspar (F) (Alberti, 1975; Koyama & Takeuchi, 1977; Concepcion-Rosabal et al., 2005; Taaca & Vasquez Jr, 2017). The intensities of the clinoptilolite peaks in the XRD traces of HC-Z, Na-Z and Cu-Z decreased

Table 8. Cu uptake (%) of the various PNZ samples.

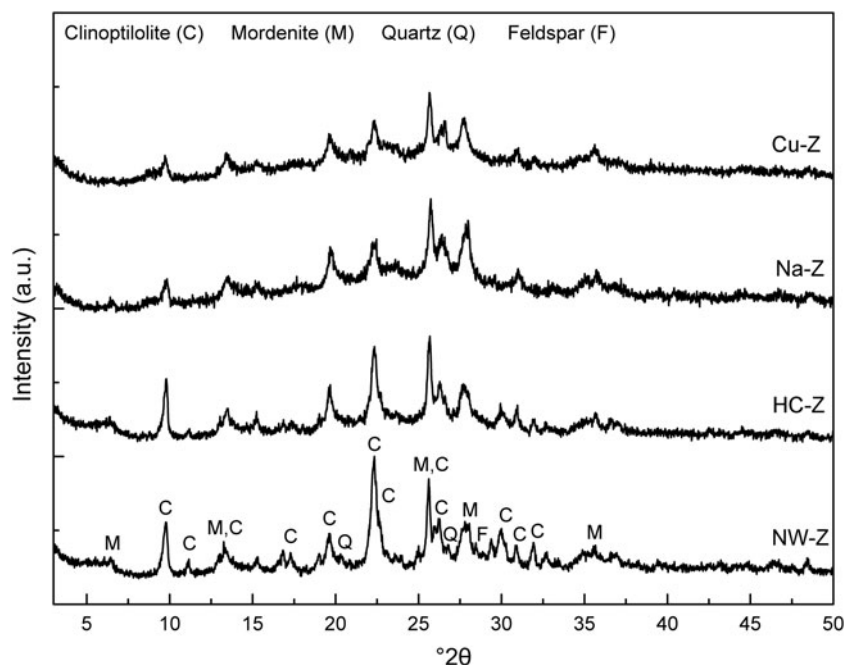| Zeolite modification	Cu uptake
NW-Z	99.44
HC-Z	96.62
Na-Z	99.88

Fig. 4. XRD traces of the NW-Z, HC-Z, Na-Z and Cu-Z samples.

compared to those of the NW-Z samples, in accordance with previous studies (Petrov, 1995; Taaca & Vasquez Jr, 2017). This is due to partial dissolution of the clinoptilolite structure after chemical modification.

Morphology of the zeolite samples. The SEM images of the NW-Z and Na-Z samples are shown in Fig. 5. The original clinoptilolite has a rough surface and consists of loose and stacked particles (Fig. 5a). The Na-Z sample has a rougher surface, which may be due to the formation of micropores after HCl treatment (Fig. 5b). Acid treatment may unclog the zeolite pores, rendering them available for adsorption (Sprynskyy *et al.*, 2005).

Discussion

Acid preconditioning was performed to remove the exchangeable cations of the zeolite framework with the H^+ ions using HCl. The acid preconditioning of the NW-Z samples was optimized by varying the particle size, HCl concentration and soaking time. The particle size and HCl concentration significantly affected the Si/Al ratio of the NW-Z samples, but these outcomes are not related. The Si/Al ratios of the HC-Z samples in Table 2 had an average value of 7.14. The CEC decreases with decreasing pH of the zeolite samples (Munthali *et al.*, 2014). The Si/Al ratio parameter may also affect the structural integrity and chemical stability of the HC-Z samples that were subjected to further modifications, including heating and ion exchange with Na^+ and Cu^{2+} cations (Whitehead, 2000; Ndayambaje, 2011). The increase in the Si/Al ratio of the HC-Z samples is due to the de-alumination process during the acid preconditioning of the samples. Further investigation of the effects of de-alumination on the PNZ samples is recommended.

The changes in the Al content of zeolites may lead to distortions in the clinoptilolite lattice, and this may affect the structural framework and the extra-framework cations (Noda *et al.*, 2008; Munthali *et al.*, 2014). Increases in the Si/Al ratios shifted characteristic infrared bands to higher wavelengths, affecting the T–O groups (Figs 1 & 2). The T–O linkages – either Al–O or Si–O –

play an important role in the electrostatic potential and binding interaction strength of cations on the negative-charge sites of the zeolite framework (Herron & Corbin, 1995; Munthali *et al.*, 2014). This resulted in the decrease in the amount of exchangeable cations and in the increase in the pore size of the HC-Z samples (Tables 5 & 6).

Zeolites should be ion-exchanged with alkalis, alkaline earth metals, transition elements or rare earth elements to generate the desired adsorbent materials (Semmens & Martin, 1988; Panayotova, 2001; Bedard, 2010). In the present work, the HC-Z samples were subjected to Na^+ exchange and subsequently soaked in $CuSO_4$ solution. The increased uptake of the Cu^{2+} ions on the zeolite samples was correlated with the Na^+ content being displaced in the framework. The PNZ samples display maximal Na^+ adsorption after 24 h. In addition, K^+ ions are mainly selected for ion exchange with Na^+. This implies that, after the acid treatment, a redistribution of cations may have occurred, where K^+ ions are more readily exchangeable compared to other native cations, such as Ca^{2+}, Mg^{2+} and Fe^{2+}.

The Na^+-loaded zeolite is the most essential form of zeolite prior to further functionalization or direct application (Semmens & Martin, 1988; Coruh, 2008). The CEC of natural zeolites increases in the presence of exchangeable Na^+ ions, making the exchange process with the target cation easier (Taaca & Vasquez Jr, 2017). In this work, the Na-Z samples were ion-exchanged with Cu^{2+} ions. The PNZ samples were able to absorb ~16.02% Cu^{2+} after exchange with Na^+ ions. Moreover, other cations, such as Ca^{2+}, Fe^{2+} and Mg^{2+}, were displaced from the zeolite structure, as was indicated by the decrease in their abundance. Hence, the synthesized Cu-Z may be used in applications such as bacterial inactivation (Olegario-Sanchez *et al.*, 2017) and gas adsorption.

The structural integrity and morphology of all of the samples were also observed in this study. No significant changes to the characteristic peaks of zeolite were detected after the acid-preconditioning technique, although the intensities of the (200) and (020) peaks of clinoptilolite in the XRD traces of the Na-Z and Cu-Z samples decreased, implying that the extra-framework species may have been redistributed or displaced (Koyama &
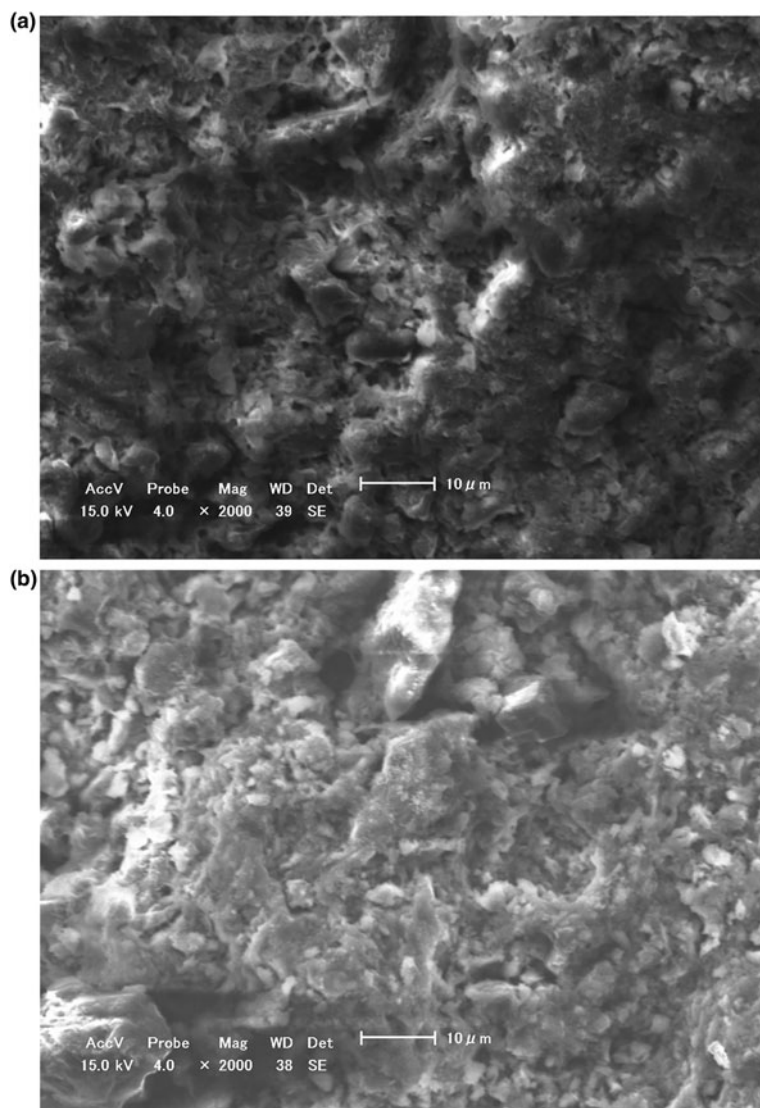
Fig. 5. SEM images of (a) NW-Z and (b) Na-Z. Scale bars: 10 µm.

Takeuchi, 1977). These variations in the extra-framework species are reflected in the SEM-EDX results (Table 5). Furthermore, no significant differences were observed in the surface features of the zeolite samples after the treatments, indicating that the preconditioning methods did not affect the surfaces of the PNZ samples. Only loose particles (NW-Z) and nanostructures (Na-Z) were observed on the zeolite surface before pretreatment and after ion exchange with Na salts.

Summary and conclusions

This work characterized the PNZs from Mangatarem, Pangasinan, Philippines, according to their compositional, phase, structural, physical and textural properties. The natural zeolite (NW-Z) was preconditioned by acid treatment (HC-Z) and Na loading (Na-Z) using HCl and NaCl, respectively. The process resulted in a decrease in Ca, Mg, Fe, K and Al cations compared with the original NW-Z sample. This change improved the properties of the PNZ samples, namely by increasing the specific surface area, the pore volume and pore size and causing minor structural changes. The most promising HC-Z samples were further

conditioned with NaCl solution to improve the Cu^{2+} uptake. The best Na-Z samples were those conditioned with 4 M NaCl for 24 h. The ion-exchange process with H^+, Na^+ and Cu^{2+} cations during pretreatment caused intensity variation in the XRD peaks of clinoptilolite in the PNZ samples. Overall, the structural integrity and surface morphology of the PNZ samples were retained, even after conducting successive pretreatments prior to direct application or further functionalization. This indicates that the PNZ samples may be used in industrial applications where improved porosity and cation selectivity may be achieved by two-step preconditioning with HCl and NaCl solutions.

References

Alberti A. (1975) The crystal structure of two clinoptilolites locality: Agoura, California, USA, Tschermaks Mineral. *Schweizerische Mineralogische und Petrographische Mitteilungen*, **22**, 25–37.

Arcilla C., Pascua C. & Alexander W. (2011) Hyperalkaline groundwaters and tectonism in the Philippines: significance to natural carbon capture and sequestration. *Energy Procedia*, **4**, 5093–5101.

Barola C., Dusaban I., Olegario-Sanchez E. & Mendoza H. (2019) The effect on the zeta potential of surface modified Philippine natural zeolites (SM-PNZ) for the adsorption of anionic solutions. *IOP Conference Series: Materials Science and Engineering*, **478**, 012039.

Bedard R. (2010) Synthesis of zeolites and manufacture of zeolitic catalysts and adsorbents: ion exchange and impregnation. Pp. 61–83 in: *Zeolites in Industrial Separation and Catalysis* (S. Kulprathipanja, editor). Weinheim, Germany, Wiley-VCH.

Cagomoc C. & Vasquez Jr M. (2016) Enhanced chromium adsorption capacity via plasma modification of natural zeolites. *Japanese Journal of Applied Physics*, **56**, 01AF02.

Cakicioglu-Ozkan, F. (2010) Effect of acid treatment on the structure of clinoptilolite. Pp. 54–55 in: *Zeolite 2010 – 8th International Conference on the Occurrence, Properties and Utilization of Natural Zeolites*. Sofia, Bulgaria: Prof. Marin Drinov Academic Publishing House.

Cakicioglu-Ozkan F. & Ulku F. (2005) The effect of HCl treatment on vapour adsorption characteristics of clinoptilolite rich natural zeolite. *Microporous and Mesoporous Materials*, **77**, 47–53.

Cerjan-Stefanović Š., Ćurković L. & Filipan T. (1996) Metal ion exchange by natural zeolites. *Croatica Chemica Acta*, **69**, 281–290.

Concepcion-Rosabal B., Rodriguez-Fuentes G., Bogdanchikova N., Bosch P., Avalos M. & Lara V. (2005) Comparative study of natural and synthetic clinoptilolites containing silver in different states. *Microporous and Mesoporous Materials*, **86**, 249–255.

Çoruh S. (2008) The removal of zinc ions by natural and conditioned clinpilolites. *Desalination*, **225**(1–3), 41–57.

Dignos E., Gabejan K., Olegario-Sanchez E. & Mendoza H. (2019) The comparison of the alkali-treated and acid-treated naturally mined Philippine zeolite for adsorption of heavy metals in highly polluted waters. *IOP Conference Series: Materials Science and Engineering*, **478**, 012030.

Doula M. & Ioannou A. (2003) The effect of electrolyte anion on Cu adsorption–desorption by clinoptilolite. *Microporous and Mesoporous Materials*, **58**, 115–130.

Garrison R., Espiritu E., Horan L. & Mack L. (1979) Petrology, sedimentology, and diagenesis of hemi pelagic limestone and tuffaceous turbidites in the Aksitero Formation, Central Luzon, Philippines. *United States Geological Survey. Professional Paper*, **1112**, 16.

Gligor D., Maicaneanu A. & Walcarius A. (2010) Iron-enriched natural zeolite modified carbon paste electrode for H_2O_2 detection. *Electrochimica Acta*, **55**, 4050–4056.

Guerrero L., Mendoza J., Ong K., Olegario-Sanchez E. & Ferrer E. (2019) Copper-exchanged Philippine natural zeolite as potential alternative to noble metal catalysts in three-way catalytic converters. *Arabian Journal for Science and Engineering*, **44**, 5581–5588.

Hernandez M. (2014) Nanoporosity and dealuminated zeolites from Mexico. Pp. 95–96 in: *Zeolite 2014 – 9th International Conference on the Occurrence, Properties and Utilization of Natural Zeolites*. Belgrade, Serbia: Institute for Technology of Nuclear and Other Mineral Raw Materials.

Herron N. & Corbin D. (1995) *Inclusion Chemistry with Zeolites: Nanoscale Materials by Design*. Dordrecht, The Netherlands, Kluwer Academic Publishers, 340 pp.

Koyama K. & Takeuchi Y. (1977) Clinoptilolite: the distribution of potassium atoms and its role in thermal stability locality: Agoura, California, USA note: z(O3) corrected. *Zeitschrift fur Kristallographie*, **145**, 216–239.

Mamba B., Nyembe D. & Mulaba-Bafubiandi A. (2009) Removal of copper and cobalt from aqueous solutions using natural clinoptilolite. *Water SA*, **35**, 307–314.

Mamba B., Nyembe D. & Mulaba-Bafubiandi A. (2010) The effect of conditioning with NaCl, KCl and HCl on the performance of natural clinoptilolite's removal efficiency of Cu^{2+} and Co^{2+} from Co/Cu synthetic solutions. *Water SA*, **36**, 437–444.

Munthali M.W., Elsheikh M.A., Johan E. & Matsue N. (2014) Proton adsorption selectivity of zeolites in aqueous media: effect of Si/Al ratio of zeolites. *Molecules*, **19**, 20468–20481.

Ndayambaje G. (2011) *Sorption Properties of Natural Zeolites for the Removal of Ammonium and Chromium Ions in Aqueous Solution*. Master's thesis. Cape Town, South Africa, University of the Western Cape.

Noda T., Suzuki K., Katada N. & Niwa M. (2008) Combined study of IRS-TPD measurement of DFT calculation on Bronsted acidity and catalytic cracking activity of cation-exchanged Y zeolites. *Journal of Catalysis*, **259**, 203–210.

Olegario E.M., Pelicano C.M.O., Dahonog L.A. & Nakajima H. (2019a) Novel ZnO nanostructures on Philippine natural zeolite (PNZ) framework designed via thermal decomposition process of solution-based $ZnCl_2$ precursor. *Materials Research Express*, **6**, 015005.

Olegario E.M., Pelicano C.M.O., Felizco J.C., Mendoza H.D. & Nakajima H. (2019b) Philippine natural zeolite surface engineered with CuO nanowires via a one-step thermal decomposition route. *Journal of the Australian Ceramic Society*, 10.1007/s41779-019-00401-y.

Olegario-Sanchez E. & Pelicano C. (2017) Characterization of Philippine natural zeolite and its application for heavy metal removal from acid mine drainage (AMD). *Key Engineering Materials*, **737**, 407–411.

Olegario-Sanchez E & Felizco J. (2017) Investigation of the structural properties of amorphous Philippine bentonite clay and its potential use for topical applications. *Key Engineering Materials*, **737**, 401–406.

Olegario-Sanchez E., Tan M., Mendoza H. & Balela M. (2017). Copper-treated Philippine natural zeolites for *Escherichia coli* inactivation. *Materials Science Forum*, **890**, 150–154.

Osonio A. & Olegario-Sanchez E (2017) Hydrophobic surface functionalization of Philippine natural zeolite for a targeted oil remediation application. *AIP Conference Proceedings*, **1901**, 080003.

Osonio A. & Vasquez Jr M. (2018) Plasma-assisted reduction of silver ions impregnated into a natural zeolite framework. *Applied Surface Science*, **432**, 156–162.

Panayotova M. (2001) Kinetics and thermodynamics of copper ions removal from wastewater by use of zeolite. *Waste Management*, **21**, 671–676.

Petrov O. (1995) Cation exchange in clinoptilolite: an X-ray powder diffraction analysis. Pp. 271–280 in: *Natural Zeolites '93: Occurrence, Properties, Use* (D. Ming & F. Mumpton, editors). Brockport, NY, USA, International Committee on Natural Zeolites.

Semmens M. & Martin W. (1988) The influence of pre-treatment on the capacity and selectivity of clinoptilolite for metal ions. *Water Research*, **22**, 537–542.

Sprynskyy M., Lebedynets M., Zbytniewski R., Namieśnik J. & Buszewski B. (2005) Ammonium removal from aqueous solution by natural zeolite, transcarpathian mordenite, kinetics, equilibrium and column tests. *Separation and Purification Technology*, **46**, 155–160.

Taaca K. & Vasquez Jr M. (2017) Fabrication of Ag-exchanged zeolite/chitosan composites and effects of plasma treatment. *Microporous and Mesoporous Materials*, **241**, 383–391.

Taaca K. & Vasquez Jr M. (2018) Hemocompatibility and cytotoxicity of pristine and plasma-treated silver–zeolite–chitosan composites. *Applied Surface Science*, **432**, 324–331.

Vargas E., Pascua C., Arcilla C., Honrado M., Alexander W., Namiki K., Fujii N., Yamakawa M., Sato T. & McKinley I.G. (2009) Origin of the Manleluag hyperalkaline hot spring, Philippines. *Geochimica et Cosmochimica Acta*, Goldschmidt Conference Abstracts, A1375.

Whitehead K. (2000) *The Application of Synthetic Zeolites for the Removal of Heavy Metals from Contaminated Effluents*. PhD thesis, Guildford, UK, University of Surrey.

Yumul G. & Dimalanta C. (1997) Geology of the Southern Zambales Ophiolite Complex, Philippines: juxtaposed terranes of diverse origin. *Journal of Asian Earth Sciences*, **15**, 4–5.